

# A New Approach for Constant DC Link Voltage in a Direct Drive Variable Speed Wind Energy Conversion System

R. Jeevajothi<sup>†</sup> and D. Devaraj<sup>\*</sup>

**Abstract** – Due to the high efficiency and compact mechanical structure, direct drive variable speed generators are used for power conversion in wind turbines. The wind energy conversion system (WECS) considered in this paper consists of a permanent magnet synchronous generator (PMSG), uncontrolled rectifier, dc-dc boost converter controlled with maximum power point tracking (MPPT) and adaptive hysteresis controlled voltage source inverter (VSI). For high utilization of the converter's power capability and stabilizing voltage and power flow, constant DC-link voltage is essential. Step and search MPPT algorithm which senses the rectified voltage ( $V_{DC}$ ) alone and controls the same is used to effectively maximize the output power. The adaptive hysteresis band current control is characterized by fast dynamic response and constant switching frequency. With MPPT and adaptive hysteresis band current control in VSI, the DC link voltage is maintained constant under variable wind speeds and transient grid currents respectively.

**Keywords:** Constant DC-link voltage, PMSG, MPPT, Step and search algorithm, Adaptive hysteresis control.

## 1. Introduction

Wind energy has considerable potential as a global clean energy source, being both widely available, though diffuse, and producing no pollution during power generation. Wind energy is currently one of the most cost-competitive renewable energy technologies. Worldwide, the cost of generating electricity from wind has fallen by more than 80 percent, and analysts forecast that costs will drop an additional 20-30 percent in the next five years.

The usage of PMSG increases energy efficiency of the whole system. Moreover PMSG has more compact mechanical structure and lower mass in comparison with conventional synchronous generator (CSG) [1]. The WECS proposed in this work is a direct drive system in which there is no gear box, maintenance costs are low, efficiency is high, noise emissions are low, and turning on system is lightweight.

Considering the usage of PMSG, three-phase diode rectifiers followed by dc-dc choppers are more economical than three-phase insulated gate bipolar transistor (IGBT) converters. In this system, the WECS does not need to synchronize its rotational speed with the grid frequency. This converter gives maximum output DC voltage. The boost converter serves to control the input dc voltage of inverters. Regardless of the dc voltage output range the diode rectifier is, the input dc voltage of inverter remains steady.

The advantage of this topology is that because of the reduction in DC link voltage ripple, the PWM characteristics are improved in comparison with diode rectifier. Also control of the DC link voltage is possible without changing generator speed [2].

Many works have analyzed the reasons of DC-link voltage fluctuation of the grid connected converter. System in [3] proposed to limit the fluctuation range of the DC - link voltage. The instantaneous generator power and grid voltage feedbacks are used to improve the dynamic response of the DC-link voltage. An adaptive carrier-based PWM method for a four-switch three-phase inverter under dc-link voltage ripple conditions is proposed [4]. The unbalanced currents which cause the oscillation at the load side can be fully overcome by using this algorithm, which compensates the dc-link voltage ripples is explained in this work.

The step and search MPPT algorithm utilised here senses the rectified voltage ( $V_{DC}$ ) alone and controls the same is used here to effectively maximize the output power maintained the DC link voltage constant under varied wind speeds.

Hysteresis band current control (HBCC) is widely used in inverters due to its simplicity in implementation, fast and accurate response. However, the main issue is its variable switching frequency which leads to extra switching losses and injection of high-frequency harmonics into the system current. To solve this problem, adaptive hysteresis current control has been introduced. Adaptive control is concerned with control law changing themselves which produces hysteresis bandwidth which results in smoother and constant switching frequency and the

<sup>†</sup> Corresponding Author: Dept. of Electrical and Electronics Engineering, Kalasalingam University, India. (rjeeva.jyothi@gmail.com)

<sup>\*</sup> Dept. of Electrical and Electronics Engineering, Kalasalingam University, India. (deva230@yahoo.com)

Received: October 20, 2012; Accepted: September 29, 2014

reduction in switching losses. The effectiveness of adaptive hysteresis band current control in inverters is demonstrated in many papers. An interior permanent magnet machine drive system with a voltage-fed current-controlled PWM inverter controlled with adaptive hysteresis band current control which maintains constant modulation frequency is presented in [5]. The work [6] presents a new hysteresis current control for three-phase systems with an R-L load and a back emf voltage. The system minimizes the switching losses by applying a short delay in the algorithm whenever the load current crosses the bands. The proposed algorithm [7] for inverter which connects distributed generation source to the grid made the output of the inverter immune to the fluctuations in the dc input voltage. In [8], a constant switching frequency current error space vector-based hysteresis controller for two-level voltage source inverter-fed induction motor (IM) drives is proposed which uses simple, fast and self-adaptive sector identification logic for sector change detection in the entire modulation range accurately eliminating the chance of introducing additional fifth and seventh harmonic components in phase current and provides harmonic spectrum of phase voltage. It is observed in [9] that for mains-connected inverter system, adaptive hysteresis current controller can provide the low switching frequency of operation of inverter switches irrespective of load variations and it ensures lower total harmonic distortion. In this paper, this scheme is utilized in maintaining the DC link voltage constant.

The proposed system uses the above features of PMSG, dc-dc boost converter, step and search algorithm and adaptive hysteresis band current controller and maintains the DC link voltage constant. The step and search algorithm maintains the DC link voltage constant by extracting maximum power from the wind turbine under varied wind speeds by generating a suitable reference voltage to the dc-dc converter. Transient grid currents affect the dc-link voltage directly. The adaptive hysteresis band current controller changes the hysteresis bandwidth according to dc-link voltage reference and maintained it constant.

## 2. Wind Turbine Characteristics

The aerodynamic rotor converts the wind power into mechanical power. The amount of mechanical power captured from wind by the turbine is given by

$$P_t = 0.5C_p(\lambda) \rho A V_w^3 \quad (1)$$

Where  $\rho$  is the air density in  $\text{Kg/m}^3$ ,  $A$  is the swept area in  $\text{m}^2$ ,  $C_p$  is the coefficient of performance of the wind turbine and  $V_w$  is the wind speed in  $\text{m/s}$ .

Fig. 1 [10] shows a group of  $C_p$ -TSR curves. Any change in the rotor speed or the wind speed induces change

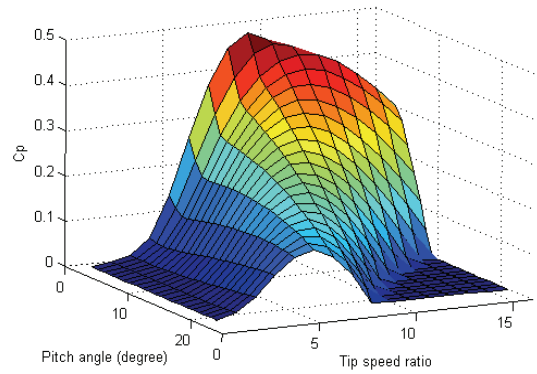


Fig. 1. Group of  $C_p$  versus  $\lambda$  characteristic

in the optimum TSR leading to power coefficient variation.

$$\lambda = \frac{R \omega_m}{V_w} \quad (2)$$

where  $\omega_m$ ,  $R$ , and  $V_w$  are the turbine rotor speed in “rad/s”, radius of the turbine blade in “m”, and wind speed in “m/s”, respectively.

## 3. Proposed Variable Speed WECS

The block diagram of the proposed variable speed WECS is illustrated in Fig. 2.

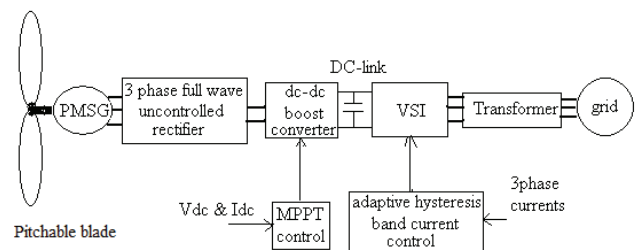


Fig. 2. Schematic diagram of the proposed variable speed WECS

The components in the proposed variable speed WECS are:

1. Wind turbine;
2. PMSG;
3. Full-wave diode bridge rectifier;
4. Boost dc-dc converter with MPPT; and
5. VSC with adaptive hysteresis band current controller.

### 3.1 PMSG

PMSGs are having large air gaps, which reduce flux linkage even in machines with multi-magnetic poles [11]. The gearbox can be omitted due to low rotational speed in the PMSG wind generation system, thus resulting in low cost. It is designed with a large diameter and small pole

pitch which increase the efficiency, reduce the weight of the active parts, and keep the end winding losses small. PMSGs have high torque density and no excitation losses.

### 3.2 Rectifier and boost dc-dc converter

This boost converter comprises an inductor, an IGBT switch, a diode and the output capacitor. MPPT extracts maximum power from the wind turbine for wind speeds from cut-in to rated, by generating a suitable reference voltage to the dc-dc converter. The reference voltage generated by the MPPT control is compared with the actual value of  $V_{DC}$  and output error value is fed to a PI controller whose output is compared to a triangular waveform. The output pulses determine the switching of dc-dc boost converter.

### 3.3 VSI with adaptive hysteresis band current controller

A VSI connected to the grid has several advantages. Grid currents can become sinusoidal with no low frequency harmonics. When connecting a VSI to a grid, an inductor must be mounted between the VSI which is operating as a stiff voltage source, and the grid, which also operates as a stiff voltage source. Inductor filters the noise which results from the fast operation of the semiconductor switches. The VSI is a standard 3-phase two-level unit, consisting of six IGBTs and antiparallel diodes. It operates in the current control mode which forces the valves to switch only when it is necessary to keep on tracking the reference of the current.

The goal of the VSI scheme is to regulate the output current. For this, an adaptive hysteresis band current controller is used. This technique exhibits constant switching frequency, better current control, easy filter design. The adaptive hysteresis band current controller assigns the switching pattern of VSI. The adaptive hysteresis band current controller operates in such a way that the amplitude of actual current is controlled to keep  $V_{DC-link}$  constant.

## 4. Control Strategy

### 4.1 Pitch control

Pitch angle control is the most common means for adjusting the aerodynamic torque of the wind turbine when wind speed is above rated speed. Pitch Control is not to optimize the generation, i.e. to work at the most efficient operating level or maximum power output level. This allows a good level of control over the angle of attack, thus control over the torque. The purpose of the control is to extend the range of operation of the wind turbine beyond the rated wind speed upto the cut-off speed. But for the control, the machine should be stopped as soon as the wind

speed reaches the rated wind speed. If the wind turbine is operated beyond the rated wind speed without stall or pitch control, the turbine will absorb more power from the wind than its capability to withstand. So, the control limits the power absorbed by the turbine from the wind to its capacity, even though much higher amount of power is available in the wind. Since the absorbed power is much less than the available power, naturally the efficiency will be less, which means that the  $C_p$  will be less or TSR is either more or less than the optimum.

Beyond rated wind speed, optimum power generation or maximum  $C_p$  cannot be expected because the intention of the controller is only to increase the grid-connected duration in a day, i.e. overall energy per day and not power at each moment. Fig. 1 clearly depicts this concept.

### 4.2 Step and search control strategy for MPPT

The step and search control strategy [12] aims at running the wind turbine at the optimum speed which gives rise to the optimum tip speed ratio (TSR) and in turn gives maximum power output. The optimum turbine speed, however, depends on the wind speed.

The control system makes use of the fact that the generated voltage and  $V_{DC}$  depend upon the speed of the turbine. Therefore, instead of sensing the turbine speed, it senses the  $V_{DC}$  and tries to control the same. The set point for this voltage is not constant. That is because the wind speed is varying every now and then which causes the optimum turbine speed to vary frequently. The set point is floating and has to be decided by trial and error method. The method is called Peak seeking. The Fig. 3 shows the step and search control strategy to track maximum power.

The strategy is to start with any arbitrary set point (A) and check what the output power is. Then give a small increment to the set point. Once again check the output at point B. If the output has increased, give an additional increment and the output once again. Incrementing by small steps should be continued till the stage (H) when the increment does not yield favourable result. At this stage, a small decrement to the set point should be given. The set point will be moving back and forth around the optimum value. Thus the power output could be maximized. In this

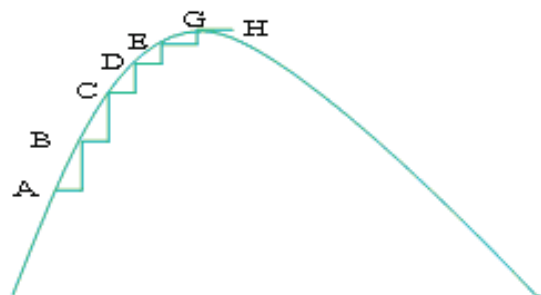


**Fig. 3.** Step and search control strategy to track maximum power

method, after giving increment to the set point, both the power output as well as the voltage level has to be checked. Four possibilities arise.

1. Power increased – voltage increased
2. Power increased – voltage decreased
3. Power decreased – voltage increased
4. Power decreased – voltage decreased

Only when power output and the voltage are increased (case 1) the set point has to be incremented. If the wind speed changes from one level to another, the turbine is not being operated at the maximum power point. The MPPT controller has to search for the new maximum power point.

### 4.3 HBCC

In the HBCC, hysteresis bands are fixed throughout the fundamental period. Hysteresis control is known to exhibit high dynamic response.

The algorithm for this scheme is given as:

$$I_{ref} = I_{max} \sin \omega t \tag{3}$$

$$\begin{cases} \text{Upper band } I_{up} = I_{ref} + h \\ \text{Lower band } I_{low} = I_{ref} - h \end{cases} \tag{4}$$

where h = Hysteresis band limit

A fixed band controller requires a reference current signal, and upper and lower bands will be obtained by adding and subtracting the hysteresis band width respectively.

$$\text{If } \begin{cases} I_a > I_{up}, V_a = -\frac{V_{dc}}{2} \\ I_a < I_{low}, V_a = +\frac{V_{dc}}{2} \end{cases} \tag{5}$$

### 4.4 Adaptive hysteresis band current control

The block diagram for adaptive hysteresis band current control of three phase grid connected VSI and its working as explained in [13] is considered here. Fig. 4 shows the adaptive hysteresis current controller concept.

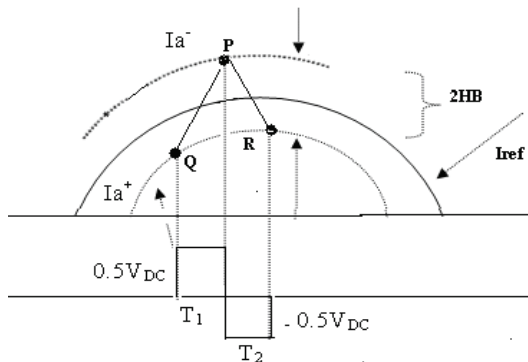


Fig. 4. Adaptive hysteresis band current controller concept

The adaptive hysteresis band current controller adjusts the hysteresis band width, according to the measured line current of the grid connected inverter. Let  $I_{ref}$  be the reference line current and  $I_{actual}$  be the actual line current of the grid connected inverter. The error signal E can be written as

$$E = I - I_{ref} \tag{6}$$

When the measured current  $I_a$  of phase A tends to cross the lower hysteresis band at point 1, then switch  $S_1$  is switched ON. When this touches the upper band at point P, switch  $S_4$  is switched ON. The expression for adaptive hysteresis bandwidth is derived as below.

$$dI_a^+ = \frac{1}{L}(0.5V_{DC} - V_a) \tag{7}$$

$$dI_a^- = -\frac{1}{L}(0.5V_{DC} + V_a) \tag{8}$$

Where L be the line inductance,  $V_a$  be the grid voltage per phase and  $V_{DC}$  be the DC link voltage. From Fig. 5. we obtain,

$$\frac{dI_a^+}{dt} T_1 - \frac{dI_{aref}}{dt} T_1 = 2HB_a \tag{9}$$

$$\frac{dI_a^-}{dt} T_2 - \frac{dI_{aref}}{dt} T_2 = -2HB_a \tag{10}$$

$$T_c = \frac{1}{f_c} = T_1 + T_2 \tag{11}$$

where  $T_1$  and  $T_2$  are the respective switching intervals and  $f_c$  is the switching frequency. Simplifying the above equations the hysteresis bandwidth (HB) is obtained as:

$$HB_a = \frac{0.125V_{DC}}{f_c L} \left[ 1 - \frac{4L^2}{V_{DC}^2} \left( \frac{V_a}{L} + m \right)^2 \right] \tag{12}$$

where  $f_c$  is modulation frequency,  $m = dI_{aref}/dt$  is the slope of command current wave. The profile of  $HB_b$  and  $HB_c$  are same as  $HB_a$  but have phase difference. According to  $(dI_{aref}/dt)$  and  $V_{DC}$  voltage, the hysteresis bandwidth is changed to minimize the influence of current distortion on modulated waveform. Thus the switching signals for the VSI are generated by the adaptive hysteresis band current controller.

### 4.5 Adaptive hysteresis band current control for maintaining constant dc link voltage

The energy loss due to conduction and switching power losses associated with the diodes and IGBTs of the inverter, tend to reduce the value of  $V_{DC}$  across capacitor  $C_{DC}$ . But

the dc link voltage should be controlled and kept at a constant value to maintain the normal operation of the inverter.

Any change in the load affects the dc-link voltage directly. The sudden removal of load would result in an increase in the dc-link voltage above the reference value, whereas a sudden increase in load would reduce the dc-link voltage below its reference value.

Generally, PI controller is used to maintain the dc-link voltage. It uses the deviation of the capacitor voltage from its reference value as its input. However, the transient response of these controllers is slow.

Instantaneous current varies ( $di/dt$ ) and Vdc voltage varies with load variations. The adaptive hysteresis band current controller changes the hysteresis bandwidth accordingly to maintain the DC link voltage constant. Also the transient response is very fast.

### 5. Results and Discussion

Simulation of the proposed utility scale variable speed WECS with PMSG and VSI with adaptive hysteresis band current control technique in tracking maximum power has been carried out using Matlab/Simulink. Simulation results are taken for two wind speeds 12 and 14 m/sec. Table 1 shows the parameters of the wind turbine model. The Table 2 shows the basic parameters used for the direct-drive generator model.

A wind turbine of 1.5 MW rating has been connected to the 1.75MVA, 2.2kV PMSG. The rating of the inverter is 1.3 MVA.

Fig.5 shows the wind speed profile. At  $t=10$ sec., wind speed is changed from 12 to 14 m/sec. in step as shown in Fig. 5.

**Table 1.** Parameters of wind turbine model

Rating	1.5MW
Blade radius	38m
No. of Blades	3
Air density	0.55kg/m <sup>3</sup>
Rated wind speed	12.4 m/sec.
Rated speed	3.07rad/sec.
Cut-in speed	4m/sec.
Cut-out speed	25m/sec.
Blade pitch angle	0 <sup>0</sup> at 12m/sec. and 4/0.7 degree/sec. at 14m/sec.
Inertia constant of turbine	0.7553 sec.

**Table 2.** Parameters of the PMSG

Rating	1.75MVA
Rated RMS line to neutral voltage	1.269kV
Rated RMS line current	0.445kA
Number of poles	4
Base angular frequency	171.98rad/sec.
Inertia constant of generator	0.3925 sec.
Stator resistance	0.003 Ω
Stator inductances	0.02μH

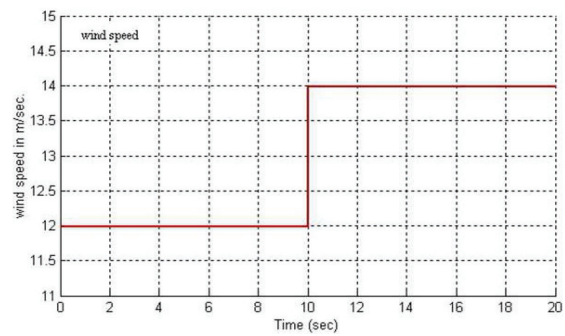


**Fig. 5.** Wind speed profile

#### 5.1 Effect of pitch control

In this work, since 12.4 m/sec. is the rated wind speed, at 12m/sec., pitch angle need not be activated. During this period,  $C_{p,max}$  is obtained as 0.44. At  $t=10$  sec., as the wind speed is 14m/sec., which is above rated wind speed of 12.4 m/sec., pitch control is activated. As the wind speed increases, the power generated by the wind turbine also increases. Once the maximum rating of the power converter is reached, the pitch angle is increased (directed to feather) to shed the aerodynamic power.

Here the pitch rate is chosen to be 4/0.7 degree/s. That is, the pitch angle can be ramped up at 4 degrees per second and it can be ramped down at 0.7 degrees per second.

The hysteresis rpm is chosen to be 2% of the maximum rpm. Small changes in pitch angle can have a dramatic effect on the power output.  $C_p$  has changed to 0.39 at 14m/sec. as shown in Fig. 6.

Fig. 7 shows the variation of tip speed ratio with time. From this figure, it is observed that the turbine speed is well controlled to maintain a optimum tip speed ratio of 7 from 0 to 10 sec. at wind speed=12m/sec. When wind speed is increased to 14m/sec., the optimum TSR is normally higher than the value at 12m/sec., but due to pitch control, it is kept at 7 itself. In general, three bladed wind

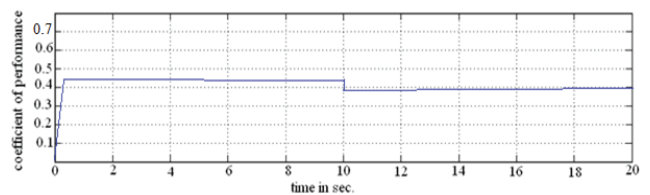


**Fig. 6.** Coefficient of Performance

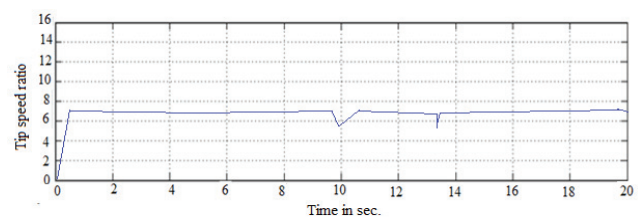


**Fig. 7.** Tip speed ratio

turbines operate at a TSR of between 6 and 8, with 7 being the most widely reported value [14].

This indicates that the turbine speed is well controlled to maintain a optimum tip speed ratios to capture maximum energy. It shows that the MPPT controller is able to track maximum power and keep  $C_p$  of the wind turbine very close to maximum Betz's coefficient of 0.593. It is the maximum fraction of the power in a wind stream that can be extracted.

### 5.2 Results of constant DC link voltage control with MPPT at wind speeds of 12 m/. and at 14 m/sec.

Simulation results of generator phase voltage and generator phase current at 12 m/sec. with zooming between 0.2 to 0.4 sec. are shown in Figs. 8(a ) and Fig. 8( b).

The Figs. 9(a) and Fig. 9(b) show the generator phase voltage and generator phase current at 14 m/sec.

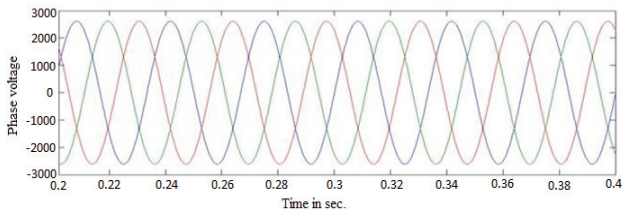


Fig. 8(a). Generator phase voltage at 12m/sec.

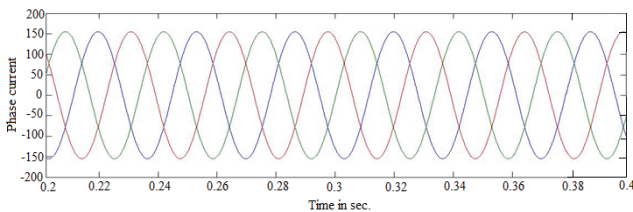


Fig. 8(b). Generator phase current at 12m/sec.

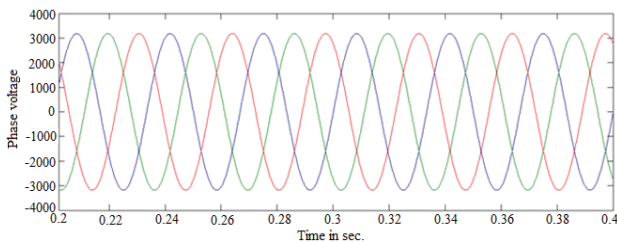


Fig. 9(a). Generator phase voltage at 14m/sec.

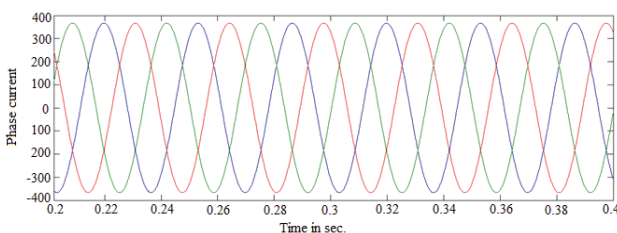


Fig. 9(b). Generator phase current at 14m/sec.

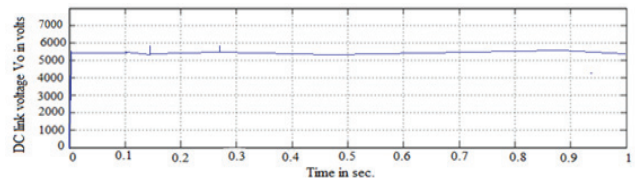


Fig. 10(a). DC link voltage at 12m/sec. and 14 m/sec.

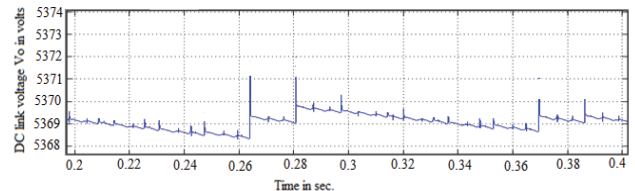


Fig. 10(b). DC link voltage at 12m/sec. and 14 m/sec (with zooming).

At 12m/sec., the generator rms phase voltage is 1.8kV and generator rms phase current is 111.1 A. At 14m/sec., the generator rms phase voltage is 2.2kV and generator rms phase current is 265.25 A. The power output at 14m/sec. is higher than at 12m/sec. So with increase in wind speed, power output of wind generator has increased.

With MPPT control under both wind speed conditions, the switching signals to boost converter are controlled in such a way that DC link voltage across  $C_o$  is maintained constant which is shown in Fig.10.

Fig. 10(a) shows the DC link voltage from  $t= 0$  to 1 sec. Simulation result with zooming from 0.2 to 0.4 sec. is shown in Fig. 10(b).

In this described WECS with MPPT, it is possible to obtain a DC link voltage of 5.369kV under both the wind speed conditions.

### 5.3 Results of constant DC link voltage control with adaptive hysteresis band current controller at load currents of 45A and 130A

To analyse the dynamic response of adaptive hysteresis current controller, the grid current is increased from 45A to 130A by applying load. The adaptive hysteresis current controller acts under this condition and made the load current to track the reference current command at a faster rate and avoided the grid waveforms getting distorted. The Fig. 11 shows the grid voltage at the point of common coupling.

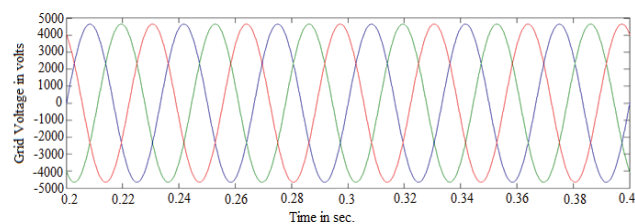


Fig. 11. Grid voltage

Figs. 12 (a-e) show the grid rms current of 45A and inverter output rms phase current, corresponding hysteresis band and DC link voltage at 45A of grid current.

With adaptive hysteresis current controller, it is possible to maintain a DC link voltage of 5.369kV which is the value maintained with MPPT algorithm in dc-dc converter under variable wind speeds. In order to prove the

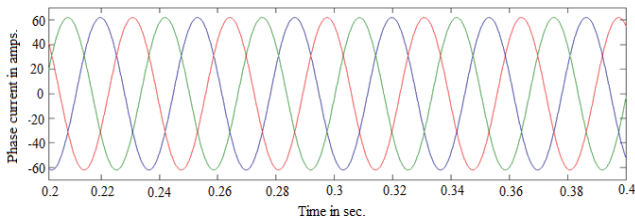


Fig. 12 (a). Grid current

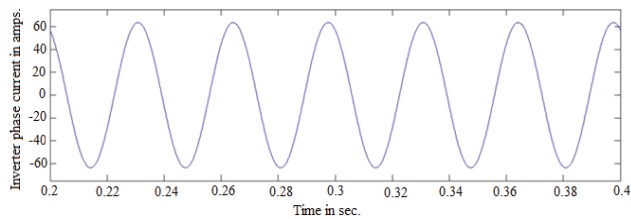


Fig. 12 (b). Inverter output phase current

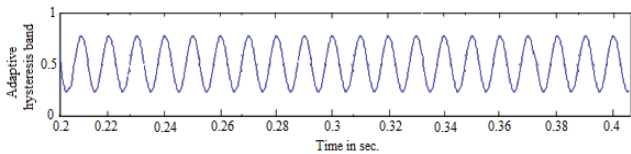


Fig. 12 (c). Adaptive Hysteresis band at 45 A

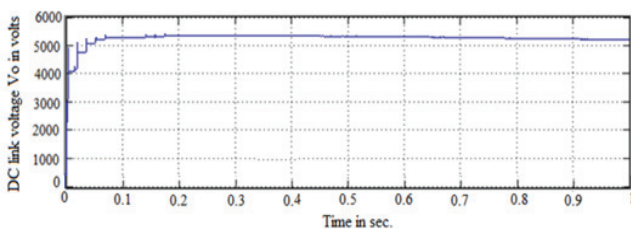


Fig. 12 (d)i. DC link voltage at 45 A with adaptive hysteresis current controller

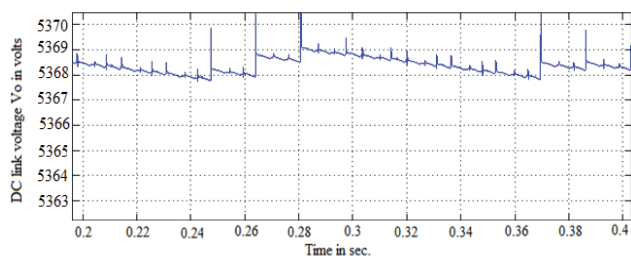


Fig. 12 (d)ii. DC link voltage at 45 A with adaptive hysteresis current controller (with zooming)

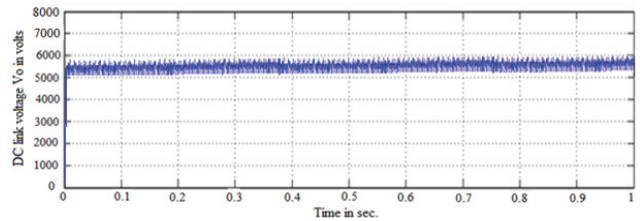


Fig. 12 (e) i. DC link voltage at 45 A with HBCC

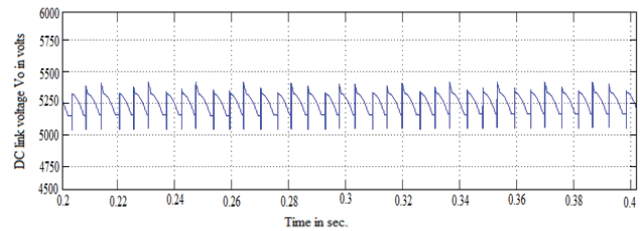


Fig. 12 (e)ii. DC link voltage at 45 A with HBCC (with zooming)

effectiveness of proposed algorithm, the DC link voltage output with adaptive hysteresis current controller is compared with HBCC.

The DC link voltage output with HBCC at 45 A is shown below in Fig. 12 (e).

The HBCC results in uneven and random switching pattern which leads to additional stress on switching devices and difficulty in designing input filters and current ripple is relatively large. It leads to extra switching losses which creates power losses and some part dissipates as heat losses also. The HBCC fixes the upper and lower bands only by a reference current signal not by the Vdc across capacitor Cdc. The HBCC is not able to maintain the target Vdc value according to the transient load conditions.

From Fig. 12(e) it is observed that, with HBCC, it is possible to obtain a DC link voltage of only 5.25kV. Also the result is not of smooth form.

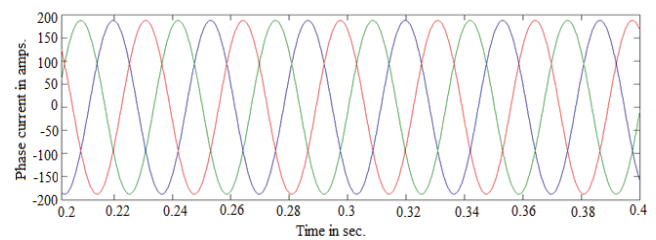


Fig. 13 (a). Grid current

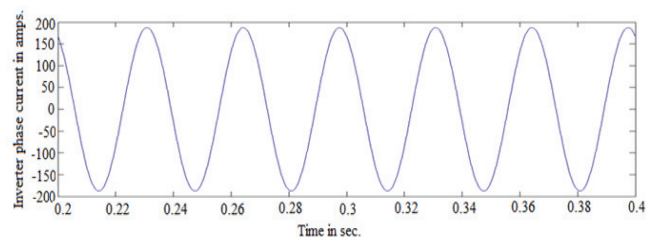


Fig. 13 (b). Inverter output phase current

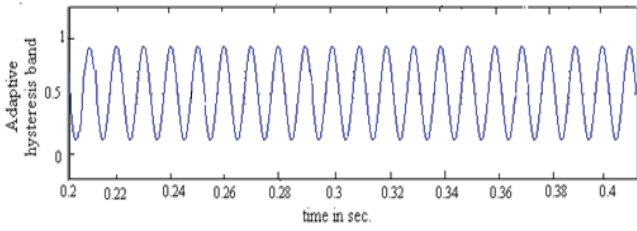


Fig. 13 (c). Adaptive hysteresis band at 130A

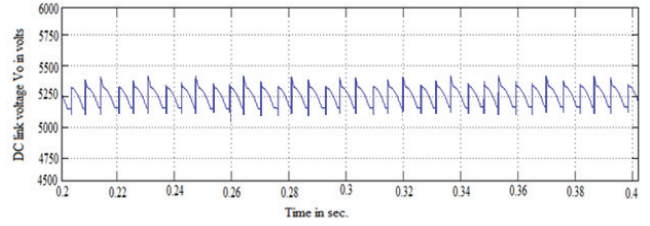


Fig. 13 (e) ii. DC link voltage at 130 A with HBCC (with zooming)

Figs. 13 (a-d) show the grid current of 130A and inverter output rms phase current, corresponding hysteresis band and DC link voltage at 130A of grid current.

As indicated in Figs. 12(c) and 13(c), the adaptive hysteresis band is varied according to the variation in load in order to maintain the constant switching frequency of operation.

Fig. 14(a and b) depict the THD value of grid current 45A and 130A respectively. It reveals that adaptive hysteresis controller gives less THD (2.76% & 2.69%) of grid current 45A and 130A respectively.

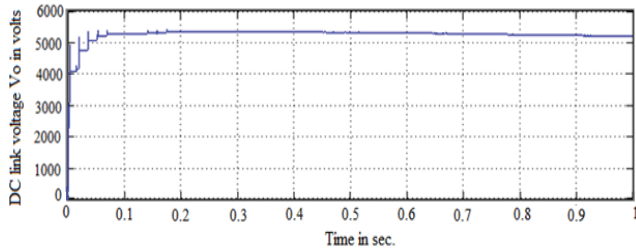


Fig. 13 (d)i. DC link voltage at 130A

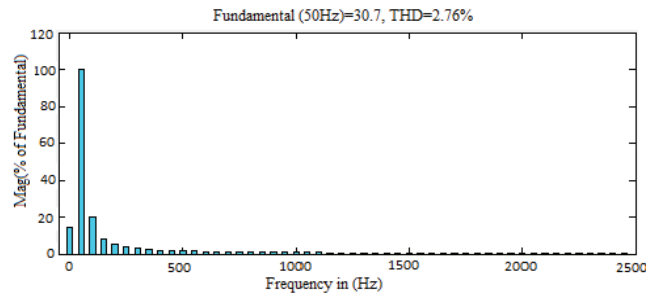


Fig. 14 (a). THD of grid current 45A

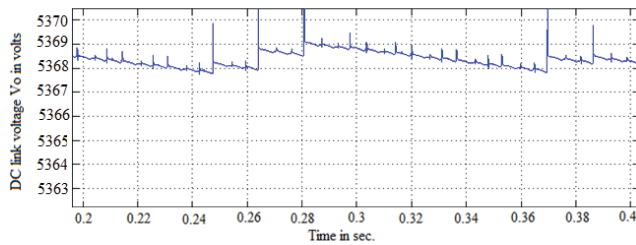


Fig. 13 (d)ii. DC link voltage at 130A (with zooming)

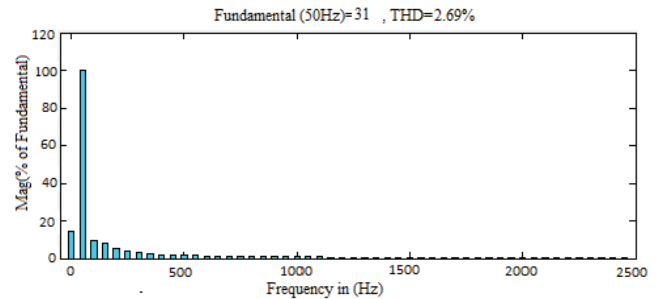


Fig. 14 (b). THD of grid current 130A

The DC link voltage output with HBCC at 130A is shown in Fig. 13 (e).

From Fig. 12(e) and Fig. 13(e), with HBCC, under both load conditions it is able to maintain a constant DC link voltage of 5.25kV but it is lesser than the DC link voltage 5.369 kV maintained with adaptive hysteresis current controller and also a smooth waveform is not obtained.

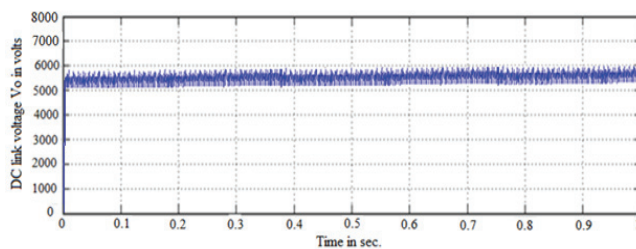


Fig. 13 (e) i. DC link voltage at 130 A with HBCC

## 6. Conclusion

This paper described a constant DC-link voltage control by a variable speed WECS with PMSG, uncontrolled rectifier, MPPT controlled dc-dc boost converter and adaptive hysteresis controlled VSI. MPPT algorithm sensed the rectified voltage ( $V_{DC}$ ) alone and controlled the same is used to effectively maximize the output power. The WECS has been simulated for 12m/sec. and 14m/sec with MPPT algorithm and maintained the DC link voltage constant. Simulation results also have shown that the proposed set up is effective in tracking the maximum power from variable voltage; variable frequency source. The adaptive hysteresis band current control is characterized by fast dynamic response and constant switching frequency. Adaptive



hysteresis band current control in VSI is tested under transient grid currents and maintained the DC link voltage constant.

### References

- [1] O. Koerner, J.Brand and K. Rechenberg “Energy Efficient Drive System for Diesel Electric Shunting Locomotive,” in *Proceedings of PEA conference, 2005*, 10, pp. - p.10.
- [2] Jamal A. Baroudi, Venkata Dinavahi and Andrew M. Knight, “A review of power converter topologies for wind generators,” *Renewable Energy*, vol. 32, pp. 2369-2385, Jan.2007.
- [3] Weihao Hu, Yue Wang, and Zhaoan Wang “An Improved DC-Link Voltage Control Method for Multiple Grid Connected Converter in Direct Drive Wind Power Generation system,” in *Proceedings of APEC conference, 2009*, pp.1939-1944.
- [4] Tuyen D. Nguyen, Hong-Hee Lee, Hoang M. Nguyen, “Adaptive Carrier-based PWM for a Four-Switch Three-Phase Inverter under DC-link Voltage Ripple Conditions,” *Journal of Electrical Engineering & Technology*, vol. 5, pp. 290-298, Mar. 2010.
- [5] K. Bose, “An adaptive hysteresis-band current technique of a voltage-fed PWM inverter for machine drive system”, *IEEE Trans. on Industrial Electronics*, vol. 37(5), pp. 402-408, Oct.1990.
- [6] Zare, Firuz and F. Ledwich, Gerard, “A New Hysteresis Current Control for Three-phase Inverters Based on Adjacent Voltage Vectors and Time Error,” in *Pro-ceedings of. PESC, 2007*, pp. 431-436.
- [7] P. Ghani, A.A. Chiane and H.M. Kojabadi, “An adaptive hysteresis band current controller for inverter base DG with reactive power compensation,” in *Proceedings of PEDSTC, 2010*, pp. 429-434.
- [8] R. Ramchand, K. Sivakumar, A. Das, C. Patel and K. Gopakumar, “Improved switching frequency variation control of hysteresis controlled voltage source inverter-fed IM drives using current error space vector,” *IET Power Electronics*, vol.3 , pp. 219-231,Mar. 2010.
- [9] B. Chitti Babu, Mohapatra, Mohamayee, S. Jena, Naik and Amiya, “Dynamic performance of adaptive hysteresis current controller for mains- connected inverter system,” in *Proceedings of IECR, 2010* , pp. 95-100.
- [10] Jianzhong Zhang, Ming Cheng, Zhe Chen and Xiaofan Fu, “Pitch Angle Control for Variable Speed Wind Turbines,” in *Proceedings of DRPT, 2008*, pp. 1-6.
- [11] Aarti Gupta, D.K Jai and Surender Dahiya, “Some investigations on recent advances in wind energy conversion systems,” in *Proceedings of IPCSIT, 2012*, pp. 47-52.
- [12] M. Kesraoui, N. Korichi and A. Belkadi, “Maximum power point tracker of wind energy conversion system,” *Renewable energy*, vol. 36, pp. 2655-2662, Oct.2011.
- [13] Murat Kale and Engin Ozdemir, “An adaptive hysteresis band current controller for shunt active power filter,” *Electric Power Systems Research*, vol. 73, pp. 113-119, Sep.2005.
- [14] Magdi Raghe and Adam M. Ragheb, *Fundamental and Advanced Topics in Wind Power*, University of Illinois at Urbana-Champaign, 216 Talbot Laboratory, USA , 2011, pp. 19-38.



**R. Jeevajothi** She is an Electrical and Electronics Engineer with Master Degree in Energy Engineering from Anna University and Master Degree in Marketing Management from Indira Gandhi National Open University. Also Ph.D in “Power System Stability Enhancement using Wind Turbine Generators” obtained from Kalasalingam University in October, 2014. Since 1991, she has been working in reputed Engineering Colleges in Tamilnadu, India.

Currently she is working as an Asst. Professor in the Department of Electrical and Electronics Engineering, Kalasalingam University, Virudhunagar Dt., Tamilnadu, India. She has organized 3 workshops. She has published 8 papers in International Journals and presented 8 papers in International conferences.



**D. Devaraj** He is an Electrical and Electronics Engineer with Master degree in Power System engineering and a PhD in Power System Security from IIT Madras, Chennai in 2001. Since 1994 he has been working in Kalasalingam University, Tamilnadu, India. Currently he is working as

Senior Professor and Head of the Department of Electrical and Electronics Engineering, Kalasalingam University, Krishnankoil. He has organized 6 Conferences, 8 Seminars and conducted 10 workshops. He has authored 2 text books, Power system analysis and Power system control. He has published 75 papers in Journals and presented 150 papers in conferences. He has chaired 15 technical sessions in various National and International Conferences. He is the Editorial board member of the International Journal of Adaptive and Innovative Systems and reviewer of IEEE Transaction on Fuzzy System, IEEE Transaction on System, Man, Cybernetics, IET Proceedings on Generation, Transmission & Distribution, International Journal on Electric Power & Energy Systems, Electric Power Components and Systems, Neuro computing and

Applied Soft computing Journal. He has Supervised 10 Ph.D, 2 M.S and 25 M.E Thesis. Presently, he is guiding 8 Ph.D scholars. He is the Project Director of Power System Automation Group attached to TIFAC-CORE in Network Engineering which is sponsored by DST, Government of India and Co-Investigator of the DST funded research project on CO<sub>2</sub> Sequestration in Process Industries. His research interest includes Power system optimization, Power system security, Voltage stability, Evolutionary algorithms, Neural network and Data Mining. He is a member of ISTE, CSI and IEEE. Presently, he is the Dean, Academic at Kalasalingam University, Krishnankoil.